LncRNA-AB209371 promotes the epithelial-mesenchymal transition of hepatocellular carcinoma cells

CHAOCHENG XIAO[1*], XINQIANG WAN[2*], HAIYANG YU[1], XIAOTONG CHEN[1], XIANGXIANG SHAN[3], YUFENG MIAO[4], RENGEN FAN[5] and WENZHANG CHA[5]

[1]Department of General Surgery, Yancheng City 6th People's Hospital;
Departments of [2]Geraeology and Obstetrics, [3]Geraeology, [4]Medical Oncology, and [5]General Surgery,
Yancheng City First People's Hospital, Yancheng, Jiangsu 224001, P.R. China

Received August 28, 2018; Accepted February 27, 2019

DOI: 10.3892/or.2019.7045

Abstract. The zinc finger protein Snail1 is an important factor in the regulation of the epithelial-mesenchymal transition (EMT) of hepatocellular carcinoma (HCC) cells. The present study demonstrated that the expression of Snail1 in HCC tissues was significantly higher compared with its expression in tissues adjacent to primary sites, as determined via western blotting. Furthermore, the results of a dual luciferase assay revealed that hsa-microRNA(miR)199a-5p negatively regulated the protein expression of Snail1 by binding to its 3' untranslated region. However, in a comparative analysis of primary HCC and its metastatic tissues using reverse transcription-quantitative polymerase chain reaction and western blotting, it was demonstrated that the expression of hsa-miR199a-5p and Snail1 in HCC metastatic tissues were significantly higher compared with primary lesions and an association between them identified that hsa-miR199a-5p lost its ability to negatively regulate Snail1. This result is contradictive to the fact that hsa-miR199a-5p inhibits the expression of the Snail1 protein. The present study hypothesized that the aberrant expression of long non-coding RNA was the cause of hsa-miR199a-5p inactivation based on loss of function rather than a reduction in content. The data collected in the present study confirmed the hypothesis that AB209371 binds to hsa-miR199a-5p and weakened the inhibitory effect of hsa-miR199a-5p on Snail1 expression. In addition, an *in vitro* EMT model was established in the present study by inducing HCC cells with TGF-β1. The results revealed that AB209371 silencing effectively reversed the hsa-miR199a-5p mediated inhibition of EMT by negatively regulating Snail1 protein expression. Therefore, AB209371 silencing in combination with hsa-miR199a-5p expression may serve as an effective means to inhibit EMT in HCC cells. The present study also revealed that hsa-miR199a-5p/Snail1 exhibits a dominant regulatory effect in the EMT of HCC cells via a Snail1 recovery experiment. In conclusion, to the best of our knowledge, the present study confirmed for the first time that the high expression of AB209371 is favorable for the EMT in HCC cells and may be a direct cause of hsa-miR199a-5p inactivation (an HCC metastasis suppressor). Additionally, AB209371 silencing combined with hsa-miR199a-5p overexpression may be an effective means to inhibit the metastasis of HCC and the EMT of HCC cells.

Introduction

Hepatocellular carcinoma (HCC) has one of the highest rates of incidence and mortality of all types of cancer worldwide, exhibiting as well as a low complete resection rate and a high postoperative recurrence rate (1-3), which are primarily driven by a high invasiveness and intrahepatic and/or extrahepatic metastasis (4). Fundamental research has demonstrated that epithelial-mesenchymal transition (EMT) serves a crucial role in the metastasis of HCC (5). Therefore, assessing the mechanism of HCC cell EMT is important for improving the prognosis of patients with HCC and for lengthening their survival.

As a zinc-finger protein, Snail1 binds to the E-box of the E-cadherin promoter and reduces the transcription of E-cadherin to promote EMT (6). Snail1 also indirectly activates vimentin and α-SMA to facilitate EMT (6). MicroRNAs (miRNAs) and long non-coding RNAs (lncRNAs) serve important roles in the regulation of cellular processes (7). It has been revealed that lncRNA influences the occurrence and development of tumors by regulating the expression of miRNAs, causing the dysfunction of protein encoding genes if expressed abnormally (8). The expression profile of lncRNAs in certain tumor cells differ from that in normal cells, which may contribute to tumor development (9). Therefore, assessing the interaction between miRNAs and lncRNAs may further elucidate cell structural and regulatory networks, and provide

Correspondence to: Dr Rengen Fan, Department of General Surgery, Yancheng City First People's Hospital, 166 Yu Long Road, Yancheng, Jiangsu 224001, P.R. China
E-mail: rengenf@163.com

*Contributed equally

Key words: long non-coding RNA, AB209371, hsa-miR199a-5p, Snail1, hepatocellular carcinoma, epithelial-mesenchymal transition, metastasis

scientific and clinical value. AB209371 is the lncRNA with the most differential expression among primary HCC and metastases that we found through screening and sequencing of the transcriptome. Furthermore, the level of AB209371 was found to decrease from metastases to primary HCC and then to adjacent normal tissues, suggesting that AB209371 may be involved in HCC metastases. Our present study demonstrates for the first time that AB209371 silencing suppresses EMT of HCC cells by restoring the negative regulation of Snail1 by hsa-miR199a-5p, providing a solid theoretic base for using lncRNA as target of genetic therapy for metastasis and migration of HCC as well as offering a reasonable explanation for the inactivation of miRNA in different tumors or tumors at different stages.

Materials and methods

Cell culture. MHCC97-H (SCSP-528) and HCC-LM3 (HCCC-9810) HCC cell lines were obtained from the Type Collection of the Chinese Academy of Sciences (Shanghai, China) and maintained in RPMI-1640 medium (cat. no. 11875093; Invitrogen; Thermo Fisher Scientific, Inc., Waltham, MA, USA) supplemented with 10% fetal bovine serum (FBS; cat. no. 10100147 Invitrogen; Thermo Fisher Scientific, Inc.). 293TN cells (CRL-3216) were purchased from the American Type Culture Collection (Manassas, VA, USA) and maintained in Dulbecco's Minimum Essential medium (DMEM; cat. no. 10569044; Invitrogen; Thermo Fisher Scientific, Inc.) supplemented with 10% FBS. All adherent cells were passaged via 0.25% trypsin digestion and incubated in an atmosphere of 5% CO_2 at 37˚C.

Assessment of AB209371, hsa-miR199a-5p, Snail1 protein and EMT markers in primary and metastatic HCC tissue, and adjacent normal tissue. Primary HCC tissue, metastasis tissue and adjacent normal tissue (2 cm from the primary site) were obtained from 20 patients at the Department of General Surgery, Yancheng City No. 1 People's Hospital (Yancheng, China) from December 2016 to March 2017. Whether patients had received any preoperative routine chemotherapy or not was not considered for enrollment. Detailed patient information is presented in Table I. Informed consent was obtained from all patients prior to enrollment and the ethical approval was obtained from the Ethics Committee of Yancheng City No. 1 People's Hospital. RNA was extracted from tissues using the Trizol reagent (cat. no. 15596018; Invitrogen; Thermo Fisher Scientific, Inc.) and reverse transcription-quantitative polymerase chain reaction (RT-qPCR) was performed to assess AB209371, hsa-miR199a-5p and Snail1 mRNA. Total protein was extracted from tissues using the T-PER tissue protein extraction reagent (cat. no. 78510; Pierce; Thermo Fisher Scientific, Inc.) and used for the detection of Snail1 and EMT markers, including E-cadherin, vimentin, α-smooth muscle actin (α-SMA) and matrix metallopeptidase-9 (MMP-9), via western blotting.

Construction of vectors. A small interfering RNA (siRNA) sequence (5'-GGTAACAGATGGAAATCCG-3') with complementary binding to AB209371 was selected (each; Sangon Biotech Co., Ltd., Shanghai, China). The oligonucleotide templates of siRNA were chemically synthesized and cloned into the linear pSIH1-cop green fluorescent protein (GFP) siRNA Vector (cat. no. SI501A-1; System Biosciences LLC, Palo Alto, CA, USA) which was obtained through digestion by *Bam*HI and *Eco*RI (Takara Biotechnology Co., Ltd., Dalian, China) and purification by agarose gel electrophoresis. An invalid siRNA sequence (5'-GAAGCCAGATCCAGCTTC C-3') was used as a negative control (NC). The recombinant vectors were named pSIH1-siRNA-AB209371 and pSIH1-NC, respectively.

The coding sequence of human Snail1 (NM_005985.3) was amplified using the primers 5'-GGAATTCGCCACCAT GCCGCGCTCTTTCCTCG-3' and 5'-CGGGATCCTCAG CGGGGACATCCTGAGCAGC-3', which contain an *Eco*RI cutting site and kozak sequence (5'-GCCACC-3') and a *Bam*HI cutting site, respectively, with the cDNA prepared by reverse transcription of RNA isolated from 293TN cells with a M-MLV Reverse Transcriptase kit (cat. no. 2640; Takara Biotechnology Co., Ltd.) in accordance with the manufacturer's protocol. Takara *Ex* Tap (cat. no. RR001Q; Takara Biotechnology Co., Ltd.) was utilized for the PCR procedure with the following thermocycling conditions: 35 cycles of denaturation at 94˚C for 30 sec, annealing at 55˚C for 30 sec and elongation at 72˚C for 45 sec. The PCR product was digested and cloned into the pCDH-CMV-MCS-EF1α-copGFP Cloning and Expression Lentivector (cat. no. CD511B-1; System Biosciences LLC). The recombinant vector was named pcDH-Snail1.

Luciferase reporter assay. The present study utilized TargetScan 7.1 (http://www.targetscan.org/) to predict whether a hsa-miR199a-5p binding site exists within the 3'-untranslated region (UTR) of human Snail1 mRNA. The same tool was used to predict the binding sites of hsa-miR199a-5p on AB209371. Primers that targeted the 3'-UTR of the Snail1 gene were designed such that flanking *Xba*I restriction sites were introduced into the 158 bp PCR product containing the hsa-miR199a-5p target site (5'-ACACTGG-3'). The primer sequences were 5'-GCTCTAGATCTGACCGATGTGTCT C-3' (Forward) and 5'-GCTCTAGAGAATATCAAACTG TACAT-3' (Reverse), respectively. The PCR reaction was performed using Takara *Ex* Taq (cat. no. RR001A; Takara Bio, Inc., Otsu, Japan) under the following conditions: 35 cycles of denaturation 94˚C for 30 sec, annealing at 55˚C for 30 sec and elongation at 72˚C for 10 sec. The PCR product was digested with *Xba*I (cat. no. 1093S; Takara Bio, Inc.) and cloned into the pGL3-promoter luciferase reporter vector (cat. no. E1761; Promega Corporation, Madison, WI, USA) to generate the vector pGL3-wild-type (wt)-Snail1. The hsa-miR199a-5p target site in the pGL3-wt-Snail1 vector was mutated from 5'-ACACTGG-3' to 5'-ACATCGG-3' to construct the mutated reporter vector, pGL3-mt-Snail1 using a Site Directed Mutagenesis kit (cat. no. 630701; Takara Bio, Inc.). The products of the vectors were confirmed by DNA sequencing on an ABI 3700 DNA sequencer (Applied Biosystems; Thermo Fisher Scientific, Inc.). Endotoxin free DNA was prepared in all cases. The hsa-miR199a-5p mimic (5'-CCC AGUGUUCAGACUACCUGUUCtt-3'), the hsa-miR199a-5p inhibitor (5'-GAACAGGUAGUCUGAACACUGGGtt-3') and NC (5'-CCCAGUGUUCAGACUACCUGUUCtt-3') were all chemically synthesized by Invitrogen (Thermo Fisher Scientific, Inc.).

Table I. Clinicopathological features of 20 patients with metastatic hepatocellular carcinoma.

Number	Sex	Age	TNM stage	Metastasis type
1	M	39	T2NXM1	Bone
2	F	72	T3N0M1	Lung
3	M	59	T1NXM1	Bone
4	M	49	T3N0M1	Head
5	M	68	T3NXM1	Colon
6	F	71	T3N1M1	Lung
7	M	66	T1N1M1	Colon
8	M	51	T3NXM1	Colon
9	M	62	T2N0M1	Lung
10	M	66	T3NXM1	Lung
11	F	65	T3N1M1	Stomach
12	M	47	T4N0M1	Bone
13	F	59	T3N1M1	Lung
14	M	45	T2N1M1	Stomach
15	F	62	T3N0M1	Stomach
16	M	55	T2NXM1	Bone
17	F	60	T3N0M1	Head
18	M	58	T3NXM1	Lung
19	M	62	T2N0M1	Lung
20	F	55	T4N1M1	Lung

M, male; F, female; TNM, tumor node metastasis. There are 20 pairs HCC tumors, their metastatisis and adjacent normal tissues obtained from patients in General Surgery Department of Yancheng City No. 1 People's Hospital between Dec. 2016 to Mar. 2017. Clinical stage category were ruled by 7th edition of TNM.

The number of viable 293TN cells in logarithmic phase growth were counted using a hemocytometer in conjunction with trypan blue staining at room temperature for 5 min. Viable cells were then seeded into 6-well plates ($2x10^5$ cells/well) and maintained in DMEM supplemented with 10% FBS at 37˚C for 24 h in a 5% CO_2 atmosphere. The transfection of plasmid DNA and RNA was performed using Lipofectamine 2000 (cat. no. 11668027; Invitrogen; Thermo Fisher Scientific, Inc.). Transfection of cells with 100 ng pGL-TK (cat. no. E6921; Promega Corporation) served as a reference for luciferase detection. Luciferase activity was measured using the dual luciferase reporter assay kit (cat. no. E1901; Promega Corporation) 48 h following transfection in accordance with the manufacturer's protocol the results of which were normalized to that of *Renilla* luciferase. The luciferase method was also used for observing the inhibition of hsa-miR489-3p function by AB209371 in MHCC97-H cells. The plasmid transfection and luciferase activity assay were the same as that in experiment of validation the target site.

Lentivirus packaging. One day prior to transfection, 293TN cells were seeded into 10 cm dishes (cat. no. 430167; Corning, Inc., Corning, NY, USA). pSIH1-siRNA-AB209371 (2 μg) and pPACK Packaging Plasmid mix (10 μg; cat. no. LV500A-1; System Biosciences LLC) were co-transfected using Lipofectamine 2000 in accordance with the manufacturer's protocol. The medium (DMEM with 10% FBS) was replaced with DMEM with 1% FBS. A total of 48 h later, the supernatant was harvested, cleared via centrifugation at 5,000 x g at 4˚C for 5 min and passed through a 0.45 μm polyvinylidene fluoride membrane (cat. no. IPVH00010; EMD Millipore, Billerica, MA, USA). The titer of virus was determined via gradient dilution. The packaged lentiviruses were named as Lv-siRNA-AB209371. Recombinant lentivirus Lv-NC, Lv-Snail1 and Lv-miR199a-3p was packaged under the same conditions.

Genetic intervention using a lentiviral approach. The experiment included 5 groups: A control group (without viral infection), an NC group (infected with Lv-NC), an AB209371 silencing group (infected with Lv-siRNA-AB209371), an Snail1 expression group (infected with Lv-Snail1) and an miR199a-5p expression group (infected with Lv-miR199a-5p). MHCC97-H and HCC-LM3 cells in logarithmic phase were seeded into 6-well plates at a density of $5x10^5$ cells/well. Following one day, viral solution was added at a multiplicity of infection of 10. Infection efficiency was assessed by observing and analyzing the level of GFP fluorescence 72 h following infection using a fluorescence inverted microscope (IX71; Olympus Corporation, Tokyo, Japan). Infection rate was estimated by dividing the number of cells expressing GFP by the total number of cells in each view. For statistics, five views were randomly selected and the mean was calculated. Total RNA and protein were isolated from the cells and subjected to RT-qPCR for AB209371 and hsa-miR199a-5p determination, and western blotting for Snail1 protein expression.

Effect of silencing AB209371 on hsa-miR199a-5p, Snail1 protein and EMT. Cells were divided into 9 groups: A control group (without virus infection or induction), a model group (induced by TGF-β1), an NC combined model group (infected with Lv-NC and induced by TGF-β1), an AB209371 silencing model group (infected with Lv-siRNA-AB209371 and induced by TGF-β1), a Snail1 expression model group (infected with Lv-Snail1 and induced by TGF-β1), an AB209371 silencing and Snail1 expression model group (infected with Lv-Snail1 and Lv-siRNA-AB209371, and induced by TGF-β1), a hsa-miR199a-5p expression model group (infected with Lv-miR199a-5p and induced by TGF-β1); a hsa-miR199a-5p expression AB209371 silencing model group (infected with Lv-miR199a-5p and Lv-siRNA-AB209371 and induced by TGF-β1) and a hsa-miR199a-5p expression AB209371 silencing Snail1 expression model group (infected with Lv-miR199a-5p, Lv-siRNA-AB209371 and Lv-Snail1, and induced by TGF-β1). MHCC97-H and HCC-LM3 cells in the logarithmic phase were seeded into 6-well plates at a density of $5x10^5$ cells/well and viral solution was added following 1 day of normal culture (37˚C with 5% CO_2) following. An EMT model was established by adding 10 ng/ml of TGF-β1 protein (cat. no. ab50036; Abcam, Cambridge, UK) and incubated under normal conditions (37˚C with 5% CO_2) for 48 h. Total RNA was isolated from the cells and subjected to RT-qPCR for AB209371 and hsa-miR199a-5p determination, and protein was isolated and subjected to western blotting for Snail1, E-cadherin, Vimentin and α-SMA protein expression.

Cellular proliferation and migration assay. MHCC97-H and HCC-LM3 cells were divided into four groups: A control group (without virus infection or induction), a model group (induced by TGF-β1), an NC combined model group (infected with Lv-NC and induced by TGF-β1) and an AB209371 silencing combined model group (infected with Lv-siRNA-AB209371 and induced by TGF-β1). A total of 48 h following infection, cells were trypsinized and seeded into 96-well plates at a density of $1x10^4$ cells/well. Cells were cultured under normal conditions (37˚C with 5% CO_2) and cell proliferation was determined using a Cell Counting Kit-8 (CCK-8) assay at 12, 24, 48 and 72 h time points. A total of 10 μl CCK-8 solution (cat. no. CK-04; Dojindo Molecular Technologies, Inc., Kumamoto, Japan) was added and cells were cultured under normal conditions (37˚C with 5% CO_2) for an additional 4 h prior to the measurement of absorbance at 450 nm.

Cell migration experiments were performed using the QCMTM 24-well Fluorimetric Cell Migration Assay kit (cat. no. ECM508; Chemicon International; Thermo Fisher Scientific, Inc.) according to the manufacturer's protocol. The kit uses an insert polycarbonate membrane with an 8-μm pore size. The insert was coated with a thin layer of EC Matrix™ (part of the migration assay kit) that occluded membrane pores and blocked the migration of non-invasive cells. RPMI-1640 medium (500 μl) supplemented with 10% FBS was used as chemoattractant. Cells that migrated and invaded the underside of the membrane were fixed with 4% paraformaldehyde at room temperature for 24 h. Invading cells were stained at room temperature for 10 min with 0.5% crystal violet (dilution ratio, 1:10) and counted via fluorescence and reported as relative fluorescence units (RFUs). The grouping and cell treatments were the same as aforementioned in the cell viability assay. A total of 72 h following lentiviral infection, cells were trypsinized. Viable cells were counted via 0.4% trypan blue (dilution ratio, 1:10) staining at room temperature for 5 min using a fluorescence inverted microscope (IX73; Olympus Corporation, Tokyo, Japan; Amplification factor, 1:160), seeded into the upper chamber of the transwell equipment at a density of $5x10^5$ cells/well, incubated under normal conditions (37˚C and 5% CO_2) for 48 h, with RPMI-1640 medium containing 20% FBS plated in the lower chamber. The experiment was performed with MHCC97-H and HCC-LM3 cells at the same time.

RT-qPCR. Total RNA of tissues and HCC cell lines were isolated using the Trizol Reagent (Invitrogen; Thermo Fisher Scientific, Inc.) according to the manufacturer's protocol. Samples were then reverse transcribed into cDNA using the M-MLV Reverse Transcriptase kit (cat. no. 2640; Takara Biotechnology Co., Ltd.) and oligo(dT)18 primer. The following specific primers were used: AB209371 forward, 5'-TTCCAGTGACTCCACGTGC-3' and reverse, 5'-AACTTTGGGCCTGTGCCGAAGGGT-3'; Snail1 forward, 5'-TTACCTTCCAGCAGCCCTACG-3' and reverse, 5'-AGGTCAGCTCTGCCACCCTGG-3'; β-actin forward 5'-CCTGTACGCCAACACAGTGC-3' and reverse, 5'-ATACTCCTGCTTGCTGATCC-3'. The lengths of the amplified products were 219, 183 and 211 bp, respectively. RT-qPCR was performed using a SYBR Premix *Ex* Taq kit (cat. no. RR420A; Takara Biotechnology Co., Ltd.) and the TP800 System (Takara Biotechnology Co., Ltd.). cDNA from 200 ng total RNA was used as the template. The thermocycling conditions for PCR were as follows: 40 cycles of denaturation at 95˚C for 10 sec, annealing at 60˚C for 20 sec and elongation at 72˚C for 20 sec. The mRNA levels of Snail1 and AB209371 were normalized to the expression of endogenous β-actin using the $2^{-\Delta\Delta Cq}$ method (10). For each sample, triplicate determinations were performed and the mean values were utilized for further analysis. To assess hsa-miR199a-5p, total RNA (2 μg) was used for cDNA preparation using the M-MLV reverse transcription kit (cat. no. 2640; Takara Biotechnology Co., Ltd.) in accordance with the manufacturer's protocol. The specific primers used were as follows: U6 snRNA: 5'-TACCTTGCGAAGTGCTTAAAC-3' and hsa-miR199a-5p: 5'-GTCGTATCCAGTGCGTGTCGTGGAGTCGGCAATTGCACTGGATACGACGCTGCC-3'. The following PCR primers were utilized: U6 forward, 5'-GTGACATCACATATACGGCAGC-3' and reverse, 5'-GTCGTATCCAGTGCGTGTCGTG-3'; hsa-miR199a-5p forward, 5'-GTGCTCGCTTCGGCAGCACAT-3' and reverse, 5'-TACCTTGCGAAGTGCTTAAAC-3'. Takara SYBR Premix Ex Tap was utilized for the PCR procedure with the following thermocycling conditions: 40 cycles of denaturation at 95˚C for 10 sec, annealing at 60˚C for 20 sec and extension at 72˚C for 20 sec. The relative level of hsa-miR199a-5p was analyzed using the $2^{-\Delta\Delta Cq}$ method, with all values being normalized to that of U6 (10).

Detection of protein contents in cells and tissues. Total protein was extracted from HCC cells or tissues using the M-PER mammalian protein extraction reagent (cat. no. 78501; Pierce; Thermo Fisher Scientific, Inc.) and the T-PER tissue protein extraction reagent (cat. no. 78510; Pierce; Thermo Fisher Scientific, Inc.), respectively. Protein was determined using the bicinchoninic acid protein assay kit (cat. no. A53227; Pierce; Thermo Fisher Scientific, Inc.). Equal quantities of protein (15 μg/lane) were then loaded onto 11% SDS-PAGE gels and transferred onto nitrocellulose membranes. Membranes were subsequently blocked with 5% bovine serum albumin (cat. no. 37520; Thermo Fisher Scientific, Inc.) in tris-buffered saline at and room temperature for 1 h and probed with monoclonal antibodies against human Snail1 (cat. no. sc-271977; 1:400), Vimentin (cat. no. sc-6260; 1:300), α-SMA (cat. no. sc-53015; 1:200), E-cadherin (cat. no. sc-8426; 1:450), MMP-9 (cat. no. sc-13520; 1:400) and β-actin (cat. no. sc-81178; 1:1,000; all, Santa Cruz Biotechnology, Inc., Dallas, TX, USA) at 4˚C for 12 h. Samples were then treated with secondary horseradish peroxidase-conjugated anti-mouse and rabbit antibodies (cat. nos. sc-516102 and sc-2370; Santa Cruz Biotechnology, Inc.; 1:3,000) at 4˚C for 4 h. Following washing, the bands were detected via chemiluminescence (Pierce; Thermo Fisher Scientific, Inc.) and imaged with X-ray films (Kodak, Rochester, NY, USA). β-actin was used as an endogenous reference for normalization. Relative optical densities were analyzed using image processing software Total Lab v1.10 (Total Laboratory Services Ltd., Blandford Forum, UK).

Statistical analysis. Data are presented as the mean ± standard deviations of three independent experiments. All statistical data were analyzed using SPSS GradPack version 20.0

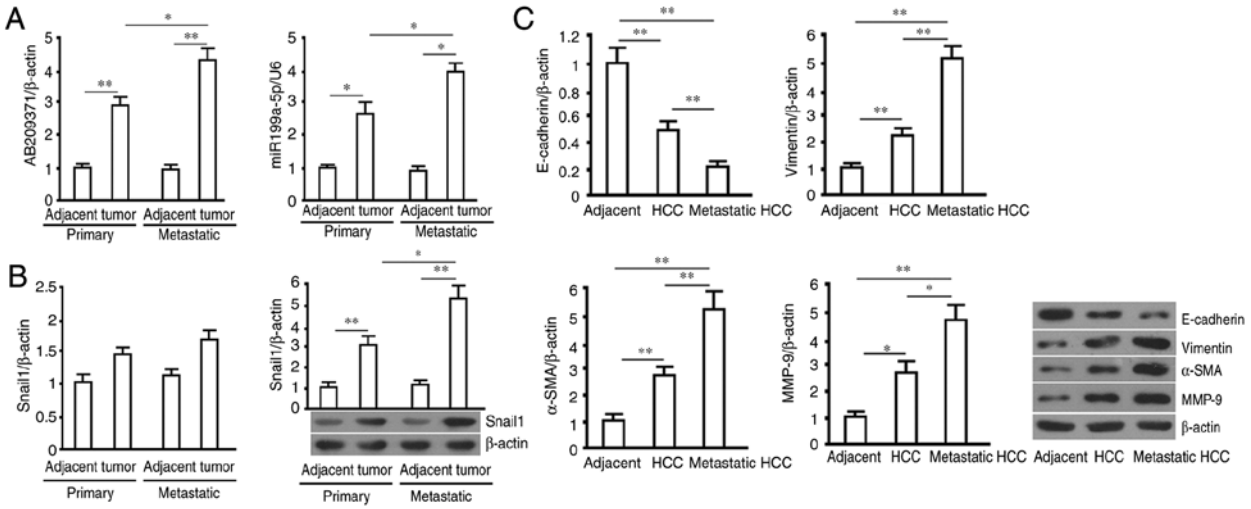

Figure 1. RT-qPCR (AB209371, hsa-miR199a-5p and Smail1 mRNA) and western blot analysis (Sanil1, E-cadherin, Vimentin, α-SMA and MMP-9) was performed using primary and metastatic HCC tumors, and adjacent normal tissue. (A) Relative levels of AB209371 and hsa-miR199a-5p, with β-actin and U6 as internal controls. (B) Snail1 mRNA and mRNA and protein levels determined via RT-qPCR and western blotting, respectively. β-actin was utilized as the internal control. (C) Protein levels of E-cadherin (116 kDa), Vimentin (55 kDa), α-SMA (37 kDa) and MMP-9 (92 kDa) were determined via western blotting and subsequent quantification with β-actin (43 kDa) as the internal control. All data are expressed as the mean ± standard deviations (sample size, n=20). *P<0.05 and **P<0.01. RT-qPCR, reverse transcription-quantitative polymerase chain reaction; miR, miRNA; α-SMA, α-smooth muscle actin; MMP-9, matrix metallopeptidase-9; HCC, hepatocellular carcinoma.

statistical software (IBM Corp., Armonk, NY, USA) and GraphPad Prism 7.0 software (GraphPad Software, Inc., La Jolla, CA, USA). Comparisons between groups were made using the Student's t-test. P<0.05 was considered to indicate a statistically significant difference.

Results

Assessment of AB209371, hsa-miR199a-5p, Snail1 mRNA and protein levels in primary HCC and metastatic HCC tissues. The relative levels of AB209371 and hsa-miR199a-p in primary and metastatic HCC tissues were significantly increased compared with adjacent normal tissue (P<0.01 and P<0.05). Furthermore, compared with primary HCC tissues, these were expressed at higher levels in HCC metastatic tissue (P<0.05; Fig. 1A). Additionally, Snail1 protein was expressed at higher levels in primary and metastatic HCC tissue compared with adjacent normal tissue (P<0.01), with an increased expression in HCC metastatic tissue compared with that of primary HCC tissue (P<0.05). The results of Snail1 mRNA assessment demonstrated that there were no marked differences between the four groups of tissue (Fig. 1B). The present study detected EMT-associated proteins in primary and metastatic HCC tissue, and in adjacent tissue. The results revealed an increase in vimentin, α-SMA and MMP-9 in primary and metastatic HCC tissue compared with adjacent tissues (P<0.01 in vimentin and α-SMA, P<0.05 in MMP-9), with the increase in metastatic tissue being more significant than the primary HCC tissue (P<0.01 in vimentin and α-SMA, P<0.05 in MMP-9). The reverse trend was observed in E-cadherin in the three tissues (Fig. 1C).

hsa-miR199a-5p binds to the Smail1 3'-UTR, which is influenced by AB209371. Bioinformatics analysis identified a seven-based hsa-miR199a-5p seed sequence in the 3miR199a-5Snail1 mRNA. The present study therefore constructed luciferase reporter vectors to verify whether this site represents a valid hsa-miR199a-5p target. The reporter vectors contained wild-type Snail1 three vectors in which the hsa-miR199a-5p target site within the 3'-UTR had been mutated. Each reporter construct expressed luciferase at a high level when compared with the untransfected group. However, miR199a-5p mimics significantly inhibited the luciferase activity of cells transfected with the reporter vector encoding the wild-type 3ithin the 3'-UTR had been mutated (P<0.01; Fig. 2A). Furthermore, the miR199a-5p inhibitor significantly increased the luciferase activity of pGL3-wt-Snail1 transfected cells (39.55±3.01 vs. 81.22±10.85; P<0.01; Fig. 2A). Conversely, in cells transfected with the reporter vector encoding the mutated hsa-miR199a-5p target site (pGl3-mt-Snail1), neither the miR199a-5p mimics nor the miR199a-5p inhibitor demonstrated any marked effect on the luciferase activity. Additionally, the co-transfection of miR199a-3p-NC (non-targeting control) had no effect on the luciferase activity of either of vector (Fig. 2A). miR199a-5p mimics were also revealed to lose their ability to inhibit luciferase expressed by the wt luciferase reporter vector in MHCC97-H cells (Fig. 2B). However, the inhibitive ability of mimics was regained following AB209371 silencing. In addition, the theoretical binding sites of hsa-miR199a-5p and AB209371 were predicted using the bioinformatics software 'TargetScan'. The results revealed that there were 11 theoretical binding sites of hsa-miR199a-5p on AB209371, which were distributed along the length of the 700 bp sequence (Fig 2B).

Effect of silencing AB209371 using the lentiviral approach on hsa-miR199a-5p and Snail1 protein in HCC cells. Recombinant lentiviruses (Lv-NC, Lv-siRNA-AB209371, Lv-Snail1 and Lv-miR199a-5p) were used to infect MHCC97-H cells. The results revealed that GFP was detected in the majority of cells

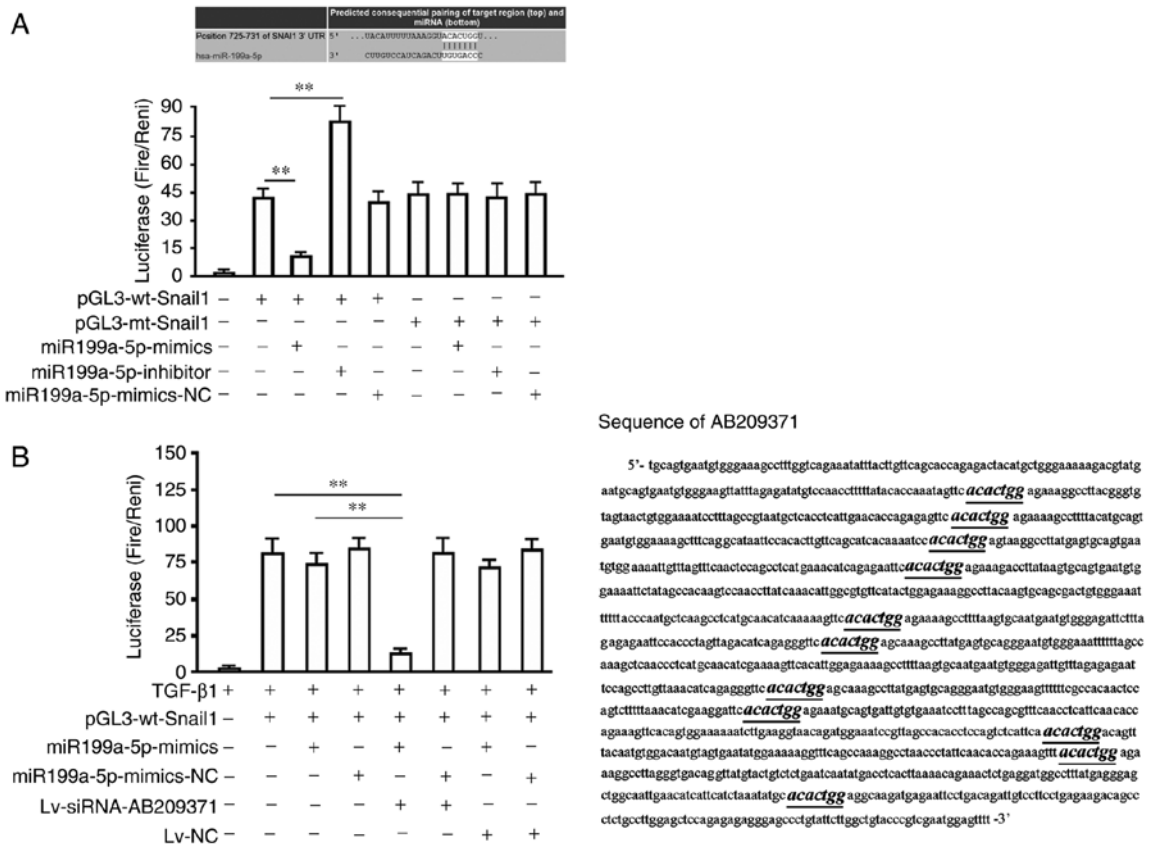

Figure 2. Luciferase assay results. (A) Predicted binding site of hsa-miR199a-5p in the 3'-UTR of the Snail1 gene and detection of luciferase activity. Luciferase activity was detected following 48 h of co-transfection in 293TN cells. (B) Effect of AB209371 silencing on the regulation of Snail1 by hsa-miR199a-5p in MHCC97-H cells. MHCC97-H cells were transfected with the indicated vectors and subjected to a luciferase activity assay 48 h later. The binding sites of hsa-miR199a-5p in AB209371 were also predicted. Data are expressed as mean ± standard deviations of at least three independent experiments. **P<0.01. miR, miRNA; UTR, untranslated region; wt, wild-type; mt, mutant; NC, negative control; TGF-β1, transforming growth factor-β1; siRNA, small interfering RNA.

72 h following infection and the proportion of GFP-expressing cells indicated that the efficiency of gene delivery was >95% in MHCC97-H cells (Fig. 3A). Furthermore, AB209371 was significantly decreased following Lv-siRNA-AB209371 transfection (P<0.01 vs. the control group). However, no change was observed in cells infected with Lv-Snail1 or Lv-miR199a-5p. Additionally, miR199a-5p was significantly increased by Lv-miR199a-5p (P<0.01 vs. the control group), but no change was observed in cells transfected with Lv-Snail1 or Lv-AB209371. Snail1 protein levels were also significantly increased following Lv-Snail1 transfection and decreased following Lv-siRNA-AB209371 transfection (P<0.01 vs. the control group). No change was detected in cells infected with Lv-miR199a-5p (Fig 3B). The results from another HCC cell line, HCC-LM3, were the same as those for MHCC97-H (data not shown).

AB209371 silencing inhibits EMT in TGF-β1 induced HCC cells. To verify that AB209371 silencing inhibits EMT in HCC cells by restoring the negative regulation of Snail1 by hsa-miR199a-5p, an *in vitro* EMT model was constructed using 10 ng/ml TGF-β1 for induction. The results revealed that, following exposure to 10 ng/ml TGF-β1 for 48 h, vimentin and α-SMA levels were increased, and E-cadherin was decreased in MHCC97-H cells, clearly indicating EMT (Fig. 4A). An RT-qPCR assay and western blotting also revealed that AB209371 silencing reduced the TGF-β1-induced increase in AB209371 and Snail1 protein (P<0.01), but had no effect on hsa-miR199a-5p. Furthermore, the overexpression of hsa-miR199a-5p increased hsa-miR199a-5p and Snail1 protein levels in TGF-β1-induced MHCC97-H cells, but had no marked effect on AB209371. Additionally, the overexpression of Snail1 increased the expression of TGF-β1 induced Snail1 in MHCC97-H cells (P<0.05), but did not affect AB209371 and hsa-miR199a-5p (Fig. 4A and B). Western blotting for EMT marker proteins revealed that the overexpression of hsa-miR199a-5p had no significant effect on the EMT of MHCC97-H cells induced by TGF-β1. However, the overexpression of hsa-miR199a-5p combined with AB209371 silencing significantly inhibited EMT. This affect was completely reversed by overexpression of Snail1 (Fig. 4A).

Effect of AB209371 silencing on the proliferation and migration of HCC cells induced by TGF-β1. The results of the cell proliferation assay revealed that TGF-β1 induction significantly enhanced cell proliferation compared with the control group (P<0.01). Furthermore, AB209371 silencing effectively inhibited the proliferation of MHCC97-H and HCC-LM3 cells induced by TGF-β1 in the logarithmic growth phase (P<0.01 vs. the model or NC control model group; Fig. 5A). The migration assay demonstrated that TGF-β1 induction significantly enhanced the migration of the two cell lines compared with

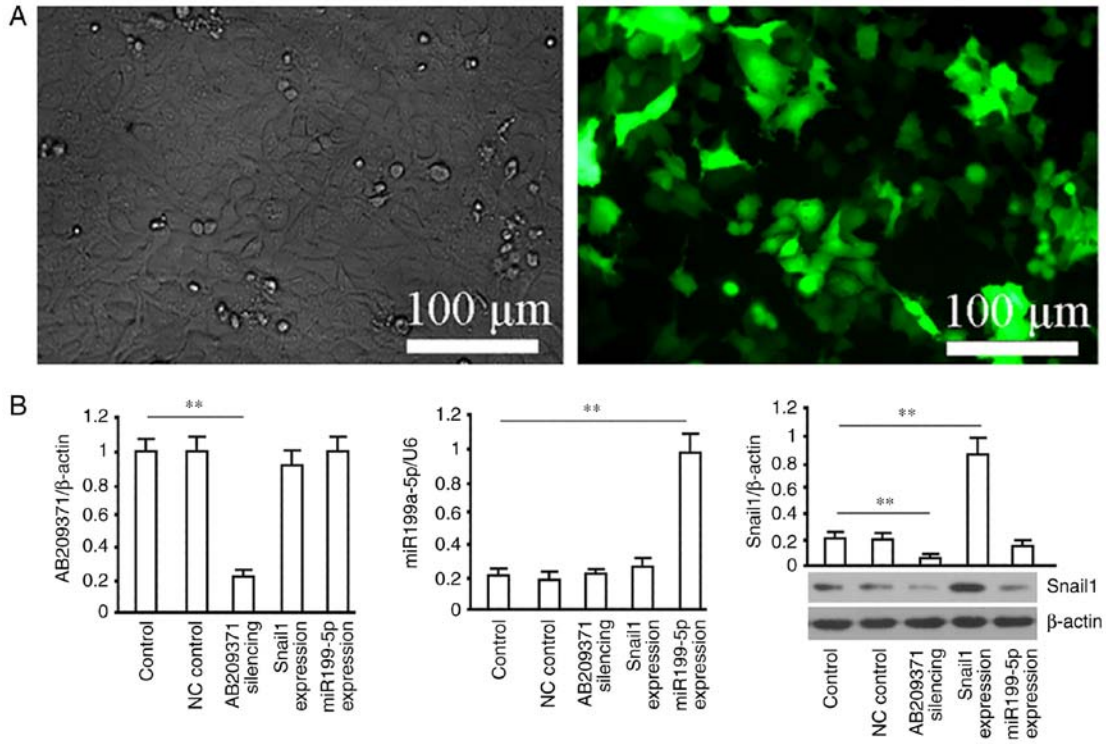

Figure 3. AB209371 silencing decreases Snail1 protein but does not affect hsa-miR199a-5p. (A) Virus infection efficiency analysis. GFP expression 72 h following MHCC97-H cell transfection with Lv-NC (scrambled siRNA to AB209371) is presented. (B) Analysis of gene intervention efficiency. AB209371 and miR199a-5p was determined via reverse transcription-quantitative polymerase chain reaction with β-actin and U6 as internal controls. Snail1 protein levels were detected via western blotting with β-actin serving as an internal reference. Each experiment was performed in triplicate and data are expressed as the mean ± standard deviation. **P<0.01.miR, microRNA; GFP, green fluorescence protein; NC, negative control.

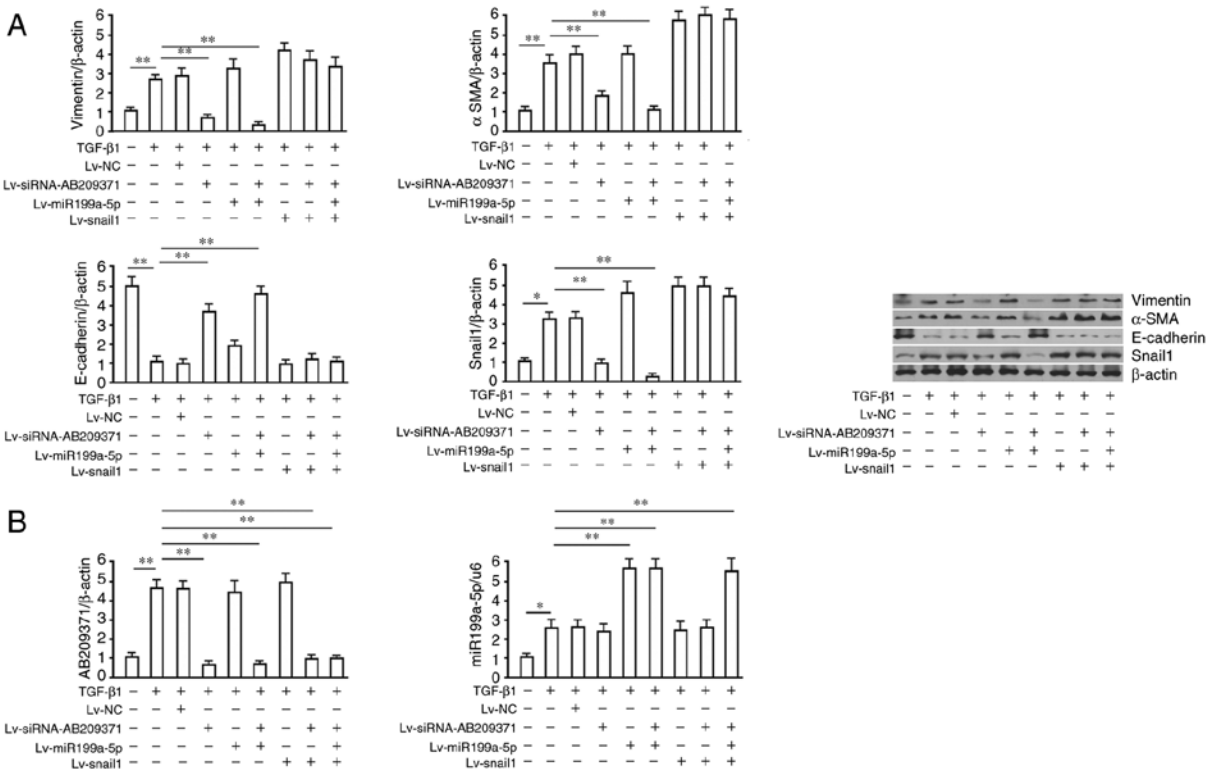

Figure 4. AB209371 silencing inhibits hepatocellular carcinoma cell EMT induced by TGF-β1 via the restoration of Snail1 inhibition by hsa-miR199-5p. (A) Western blotting of EMT markers, E-cadherin (116 kDa), Vimentin (55 kDa), α-SMA (37 kDa) and Snail1 (34 kDa) protein. A total of 24 h following MHCC97-H transfection with recombinant viruses, cells were induced with TGF-β1 (10 ng/ml) for a further 48 h. β-actin was utilized as a loading control. (B) Determination of AB209371 and hsa-miR199a-5p levels via reverse transcription-quantitative polymerase chain reaction. Data are representative of at least three independent experiments and are presented as the mean ± standard deviation. **P<0.01 and *P<0.05. EMT, epithelial-mesenchymal transition; TGF-β1, transforming growth factor-β1; miR, miRNA; α-SMA, α-smooth muscle actin; NC, negative control; siRNA, small interfering RNA.

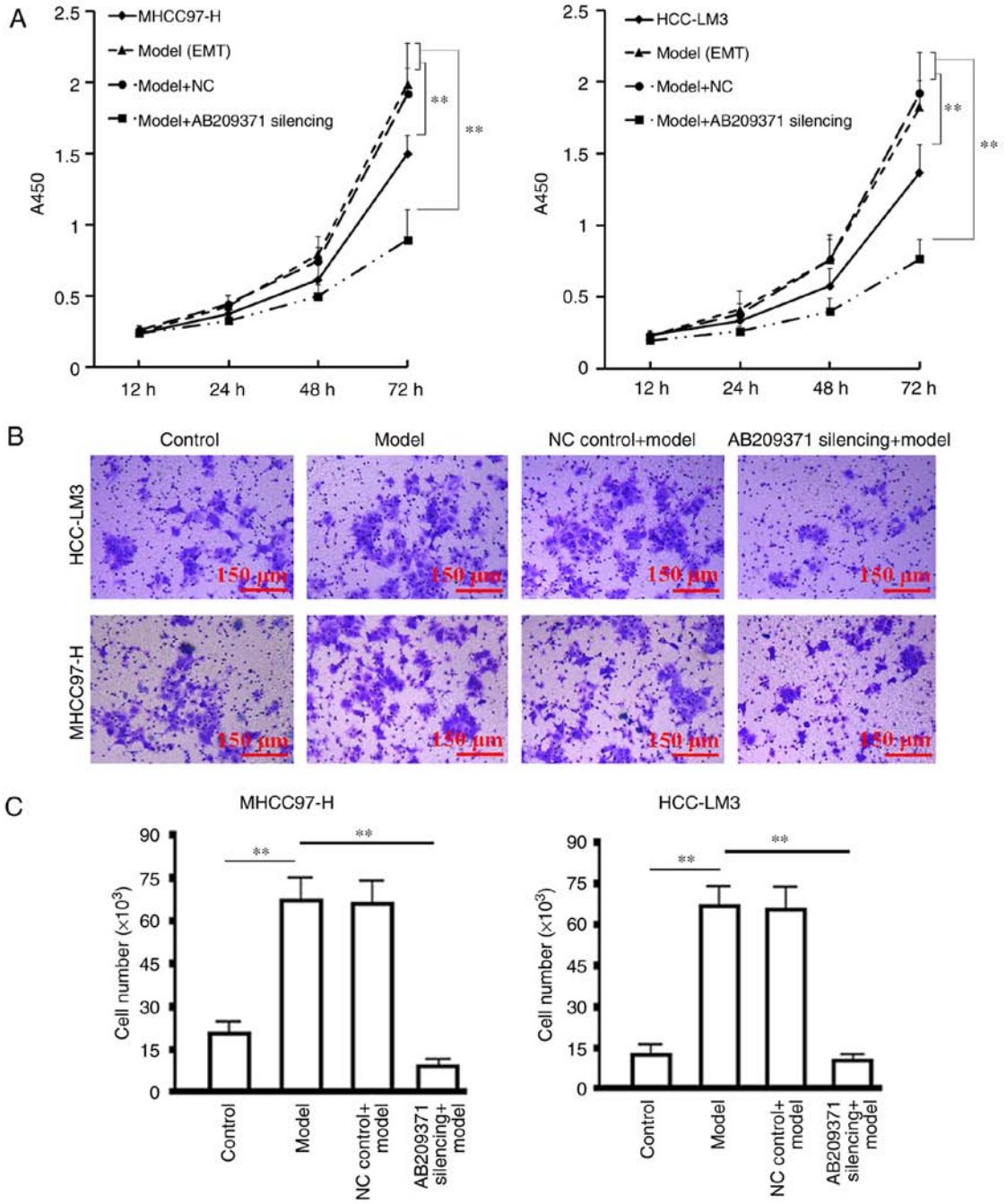

Figure 5. Effect of AB209371 silencing on the proliferation and migration of hepatocellular carcinoma cells induced by TGF-β1. (A) A cellular proliferation assay was performed 24 h following MHCC97-H and HCC-LM3 transfection with the indicated lentivirus. Samples were induced with TGF-β1(10 ng/ml), incubated for 48 h, seeded to 96-well plates and subjected to the assay for 12, 24, 48 and 72 h. Longitudinal coordinates was expressed as the absorbance value of the sample at 450 nm wavelength (A450). (B and C) Cell migration assay and statistical analysis. Images are representative. Data are expressed as the mean ± standard deviation of at least three independent experiments. **P<0.01. TGF-β1, transforming growth factor-β1; EMT, epithelial-mesenchymal transition; NC, scrambled siRNA to AB209371.

the control group (P<0.01). Furthermore, AB209371 silencing effectively inhibited cell migration (P<0.01 vs. all other groups induced by TGF-β1), which was demonstrated by the decreased number of cells that passed through the basement membrane (Fig. 5B).

Discussion

LncRNA is a class of natural DNA transcriptional products comprising >200 bases (11). LncRNA has also been determined to serve an important role in the proliferation and regulation of certain types of tumor (12,13). Studies have revealed that lncRNA and miRNA interact to regulate tumor metastasis. LncRNA can also regulate miRNAs by serving as an endogenous miRNA inhibitor that suppresses miRNA function and thus affects the malignant biological behavior of cancer cells (14). LncRNAs participate in the promotion of HCC initiation and metastasis progression, as revealed by previous studies (15,16). The invasion and metastasis of cancer involves cancer cells breaking away from the primary tumor

site, transferring to discrete tissues or remote organs and proliferating into cancer cells of the same type. This process is dependent on the interaction of cancer cells and the internal environment, which may promote their survival, growth angiogenesis, invasion and metastasis (17,18). Therefore, EMT is important for the invasion and metastasis of cancer cells (19-21). The EMT of HCC cells is closely associated with HCC metastasis and post-operative metastasis (22,23). However, the lncRNAs that are involved in the EMT of HCC cells are yet to be fully determined. Furthermore, to the best of our knowledge, the biological role and underlying mechanism of AB209371 in the EMT of HCC has not yet been reported.

As a transcription factor, Snail1 functions by binding to the E-box element of the 5'-CANNTG-3' core base sequence (N=A, T, C or G) in the promoter region of many tumor-associated genes (24,25). Snail1 can regulate the EMT of various tumors by promoting or inhibiting the transcription of E-cadherin, interleukin-8 and cluster of differentiation 147 (26,27). To verify whether Snail1 contributes to HCC metastasis, the present study tested primary and metastatic HCC samples, and adjacent normal tissues. The results revealed that the expression of Snail1 protein was significantly increased in primary or metastatic HCC tissues compared with adjacent tissues. The results also indicated that the underlying cause of this increased expression was the decrease in hsa-miR199a-5p content. The present study therefore hypothesized that a further decrease in hsa-miR199a-5p may further increase Snail1 protein expression, resulting in EMT. The present study hypothesizes that there is a mechanism which may explain these results and the results which demonstrated the weakened negative regulation of hsa-miR199a-5p on the Snail1 protein in the process of metastasis of HCC. The results of the present study indicate that the inactivation process of hsa-miR199a-5p starts from the initial stage of EMT or HCC metastasis. Based on data from previous studies, the present study hypothesizes that lncRNA may be the key factor (28), that is, a group of miRNAs are elevated and the binding of has-miR199a-5p to the 3'-UTR region of the Snail1 gene is inhibited by competitive binding. Screening was carried out based on two aspects. The present study hypothesized that the expression of hsa-miR199a-5p and Snail1 protein in HCC and its metastatic tissues revealed the following: i) hsa-miR199a-5p was elevated in metastatic tissues of HCC and may not effectively inhibit Snail1 protein expression; ii) the increased expression of Snail1 protein in HCC metastasis may be due to post-transcriptional regulation inactivation (with no change in mRNA). Based on these two facts combined with existing theories that lncRNA regulates miRNA to serve as endogenous miRNA inhibitor to suppress miRNA function (8), the present study hypothesizes that the inactivation of hsa-miR199a-5p may be caused by an increase in the content of a lncRNA and that this lncRNA must have two sets of characteristics: i) Its content in the metastatic tissues of HCC is higher than that in primary HCC; ii) it effectively inhibits the binding of hsa-miR199a-5p to the 3'-UTR of the Snail1 gene.

The experiments of the present study revealed that AB209371 was increased in primary and metastatic HCC compared with adjacent normal tissues, and was also increased to a greater degree in metastatic HCC tissues compared with primary HCC tissues, indicating that there may be an association among AB209371, EMT and HCC metastasis. The results of bioinformatics indicated that there was a 7-base seed region of hsa-miR199a-5p on the 3'-UTR of Snail1 and that there were 11 seeding regions on the 800-base AB209371. As a result, the present study hypothesized that elevated AB209371 bound to hsa-miR199a-5p as a miRNA inhibitor, disabling the negative regulation of Snail1 by hsa-miR199a-5p, meaning that Snail1 expression was increased, resulting in in HCC EMT. LncRNAs, as a competing endogenous RNAs, interact with miRNAs to regulate target genes and as such serve important roles in the EMT of HCC cells and the metastasis of HCC (29,30). The present study concluded that AB209371 silencing restores the negative regulation of Snail1 by hsa-miR199a-5p to inhibit cancer. This conclusion was based on the following results: i) hsa-miR199a-5p negatively regulated Snail1 by binding to its 3'-UTR; ii) AB209371 silencing inhibited EMT in HCC, which was reversed by the overexpression of Snail1; iii) the overexpression of hsa-miR199a-5p exhibited no marked effect on HCC EMT, but did inhibit EMT when AB209371 was silenced. Considering that Snail1 overexpressed by the lentiviral system did not contain the wild-type 3'-UTR, it would not be affected by miRNA. Therefore, the present study hypothesizes that a hsa-miR199a-5p/Snail1 pathway regulates HCC EMT. The upregulation of hsa-miR199a-5p is considered to be an intrinsic antagonistic response to HCC metastasis and elevated AB209371 may be the reason why the inhibition of HCC metastasis is unable to occur. The present study established an EMT model of HCC cell lines via induction with TGF-β1 to clarify the effect of AB209371 on the EMT of HCC cells. The present study confirmed that AB209371 silencing effectively restored hsa-miR199a-5p inhibition of hepatoma cell EMT and HCC metastasis. Furthermore, AB209371 silencing in combination with hsa-miR199a-5p overexpression was an effective method for preventing HCC metastasis by inhibiting the EMT of HCC cells. These results may aid the development of clinical personalized treatments for patients with HCC in the future. In addition, hsa-miR199a-5p was determined to negatively regulate Snail1 protein expression in several groups of stem cells and was inactivated following TGF-β1-induction. This outcome further confirms that TGF-β1 induction leads to an increase in the AB209371 content of HCC cells, which may be the key to hsa-miR199a-5p inactivation.

Although the present study systematically assessed the associations of AB209371, hsa-miR199a-5p and Snail1, further study is required to determine how the elevation of AB209371 in HCC cells occurs. However, The present study demonstrated that lncRNA may serve as a link between the EMT of HCC cells and the metastasis of HCC. The present study demonstrated for the first time that AB209371 silencing suppresses the EMT of HCC cells by restoring the negative regulation of Snail1 by hsa-miR199a-5p. These results may lay a solid theoretic base for the use of lncRNA as a target of genetic therapy for HCC metastasis and invasion.

Acknowledgements

The authors would like to thank Professor HaiXin Qian for his guidance in the design and implementation of the present study.

Funding

The present study was supported by the Jiangsu Provincial Scientific Research of 333 Project (grant no. BRA2018251) and The Yancheng Medical Science Development Foundation (grant no. YK2017007).

Availability of data and materials

The datasets used and/or analyzed during the present study are available from the corresponding author on reasonable request.

Authors' contributions

RF, CX, XW and WC supervised the present study. CX, XW, HY, XC, XS and YM performed the experiments. RF, CX, XW and WC collected the data, performed data analysis and wrote the manuscript. All authors read and approved the manuscript and agree to be accountable for all aspects of the research in ensuring that the accuracy or integrity of any part of the work are appropriately investigated and resolved.

Ethics approval and consent to participate

The study was reviewed and approved by the Yancheng City First People's Hospital Institutional Review Board (Yancheng, China).

Patient consent for publication

Written informed consent was obtained from all patients for the publication of this article and accompanying datasets.

Competing interests

The authors declare that they have no competing interests.

References

1. Mulcahy MF: Management of hepatocellular cancer. Curr Treat Options Oncol 6: 423-435, 2005.
2. Bosch FX, Ribes J, Díaz M and Cléries R: Primary HCC: Worldwide incidence and trends. Gastroenterology 127 (Suppl 1): S5-S16, 2004.
3. El-Serag HB: Hepatocellular carcinoma. N Engl J Med 365: 1118-1127, 2011.
4. Yang H, Lin M, Xiong F, Yang Y, Nie X, McNutt MA and Zhou R: Combined lysosomal protein transmembrane 4 beta-35 and argininosuccinate synthetase expression predicts clinical outcome in hepatocellular carcinoma patients. Surg Today 41: 810-817, 2011.
5. Chen JS, Li HS, Huang JQ, Zhang LJ, Chen XL, Wang Q, Lei J, Feng JT, Liu Q and Huang XH: Down-regulation of Gli-1 inhibits hepatocellular carcinoma cell migration and invasion. Mol Cell Biochem 393: 283-291, 2014.
6. Kaufhold S and Bonavida B: Central role of Snail1 in the regulation of EMT and resistance in cancer: A target for therapeutic intervention. J Exp Clin Cancer Res 33: 62, 2014.
7. Abdelmohsen K and Gorospe M: Noncoding RNA control of cellular enescence. Wiley Interdiscip Rev RNA 6: 615-629, 2015.
8. Alaei-Mahabadi B and Larsson E: Limited evidence for evolutionarily conserved targeting of long non-coding RNAs by microRNAs. Silence 4: 4, 2013.
9. Schmitt AM and Chang HY: Long Noncoding RNAs in Cancer Pathways. Cancer Cell 29: 452-463, 2016.
10. Livak KJ and Schmittgen TD: Analysis of relative gene expression data using real-time quantitative PCR and the $2^{-\Delta\Delta C_T}$ method. Methods 25: 402-408, 2001.
11. Liu H, Luo J, Luan S, He C and Li Z: Long non-coding RNAs involved in cancer metabolic reprogramming. Cell Mol Life Sci 76: 495-504, 2019.
12. Ponting CP, Oliver PL and Reik W: Evolution and functions of long noncoding RNAs. Cell 136: 629-641, 2009.
13. Bergmann JH and Spector DL: Long non-coding RNAs: Modulators of nuclear structure and function. Curr Opin Cell Biol 26: 10-18, 2014.
14. Huang JF, Guo YJ, Zhao CX, Yuan SX, Wang Y, Tang GN, Zhou WP and Sun SH: Hepatitis B virus X protein (HBx)-related long noncoding RNA (lncRNA) down-regulated expression by HBx (Dreh) inhibits hepatocellular carcinoma metastasis by targeting the intermediate filament protein vimentin. Hepatology 57: 1882-1892, 2013.
15. Noh JH and Gorospe M: AKTions by cytoplasmic lncRNA *CASC9* promote hepatocellular carcinoma survival. Hepatology 68: 1675-1677, 2018.
16. Wu LL, Cai WP, Lei X, Shi KQ, Lin XY and Shi L: NRAL mediates cisplatin resistance in hepatocellular carcinoma via miR-340-5p/Nrf2 axis. J Cell Commun Signal 13: 99-112, 2018.
17. Tsang WP, Wong TW, Cheung AH, Co CN and Kwok TT: Induction of drug resistance and transformation in human cancer cells by the noncoding RNA CUDR. RNA 13: 890-898, 2007.
18. Kulesa PM and McLennan R: Neural crest migration: Trailblazing ahead. F1000Prime Rep 7:02, 2015.
19. Maritzen T, Schachtner H and Legler DF: On the move: Endocytic trafficking in cell migration. Cell Mol Life Sci 72: 2119-2134, 2015.
20. Deng B, Zhang S, Miao Y, Zhang Y, Wen F and Guo K: Down-regulation of Frizzled-7 expression inhibits migration, invasion, and epithelial-mesenchymal transition of cervical cancer cell lines. Med Oncol 32: 102, 2015.
21. Yuan W, Yuan Y, Zhang T and Wu S: Role of Bmi-1 in regulation of ionizing irradiation-induced epithelial-mesenchymal transition and migration of breast cancer cells. PLoS One 10: e0118799, 2015.
22. Bao YX, Cao Q, Yang Y, Mao R, Xiao L, Zhang H, Zhao HR and Wen H: Expression and prognostic significance of golgiglycoprotein73 (GP73) with epithelial-mesenchymal transition (EMT) related molecules in hepatocellular carcinoma (HCC). Diagn Pathol 8: 197, 2013.
23. Zhang H, Song Y, Zhou C, Bai Y, Yuan D, Pan Y and Shao C: Blocking endogenous H_2S signaling attenuated radiation-induced long-term metastasis of residual HepG2 cells through inhibition of EMT. Radiat Res 190: 374-384, 2018.
24. Nieto MA: The snail super family of zinc-finger transcription factors. Nat Rev Mol Cell Biol 3: 155-166, 2002.
25. Cheng CW, Wu PE, Yu JC, Huang CS, Yue CT, Wu CW and Shen CY: Mechanisms of inactivation of E-cadherin in breast carcinoma: Modification of the two-hit hypothesis of turn out suppressor gene. Oncngene 20: 3814-3823, 2001.
26. Argast GM, Krueger JS, Thomson S, Sujka-Kwok I, Carey K, Silva S, O'Connor M, Mercado P, Mulford IJ, Young GD, *et al*: Inducible expression of TGFβ, Snail and Zeb1 recapitulates EMT in vitro and in vivo in a NSCLC model. Clin Exp Metastasis 28: 593-614, 2011.
27. Barnett P, Arnold RS, Mezencev R, Chung LW, Zayzafoon M and Odero-Marah V: Snail-mediated regulation of reactive oxygen species in ARCa P human prostate cancer cells. Biochem Biophys Res Commun 404: 34-39, 2011.
28. Lanzafame M, Bianco G, Terracciano LM, Ng CKY and Piscuoglio S: The role of long non-coding RNAs in hepatocarcinogenesis. Int J Mol Sci 19: E682, 2018.
29. Chen L, Wang W, Cao L, Li Z and Wang X: Long non-coding RNA CCAT1 acts as a competing endogenous RNA to regulate cell growth and differentiation in acute myeloid leukemia. Mol Cells 39: 330-336, 2016.
30. Karreth FA and Pandolfi PP: ceRNA cross-talk in cancer: When ce-bling rivalries go awry. Cancer Discov 3: 1113-1121, 2013.